Available online at www.sciencedirect.com
SCIENCE DIRECT®
Biochemical and Biophysical Research Communications 324 (2004) 269–275
BBRC
www.elsevier.com/locate/ybbrc

Advanced cancers: eradication in all cases using 3-bromopyruvate therapy to deplete ATP☆,☆☆

Young H. Ko[a,b,*], Barbara L. Smith[a], Yuchuan Wang[a], Martin G. Pomper[a], David A. Rini[c], Michael S. Torbenson[d], Joanne Hullihen[b], Peter L. Pedersen[b,*]

[a] The Russell H. Morgan Department of Radiology, Johns Hopkins University School of Medicine, Baltimore, MD 21205-2185, United States
[b] Department of Biological Chemistry, Johns Hopkins University School of Medicine, Baltimore, MD 21205-2185, United States
[c] Department of Art as Applied to Medicine, Johns Hopkins University School of Medicine, Baltimore, MD 21205-2185, United States
[d] Department of Pathology, Johns Hopkins University School of Medicine, Baltimore, MD 21205-2185, United States

Received 25 August 2004
Available online 25 September 2004

Abstract

A common feature of many advanced cancers is their enhanced capacity to metabolize glucose to lactic acid. In a challenging study designed to assess whether such cancers can be debilitated, we seeded hepatocellular carcinoma cells expressing the highly glycolytic phenotype into two different locations of young rats. Advanced cancers (2–3 cm) developed and were treated with the alkylating agent 3-bromopyruvate, a lactate/pyruvate analog shown here to selectively deplete ATP and induce cell death. In all 19 treated animals advanced cancers were eradicated without apparent toxicity or recurrence. These findings attest to the feasibility of completely destroying advanced, highly glycolytic cancers.
© 2004 Elsevier Inc. All rights reserved.

Keywords: Advanced cancers; Liver/colon cancer; Cancer therapy; 3-Bromopyruvic acid; ATP depletion

Cancer is frequently asymptomatic reaching an advanced stage where treatment options are limited, e.g., liver cancer [1]. Significantly, such cancers frequently exhibit a highly glycolytic phenotype [2,3] dependent on the expression of hexokinase II [4]. In fact, it has been demonstrated that human liver cancers derived from metastatic colorectal cancer express enhanced levels of this enzyme [5]. Although the highly glycolytic phenotype has provided the basis for an emerging technique for cancer detection [6], i.e., FDG-positron emission tomography, it has not been widely exploited as a therapeutic target with the mitochondria for facilitating ATP depletion and cancer destruction. Here, we report how advanced cancers can be selectively destroyed using this approach.

Materials and methods

Cell source, passage, culture, and viability or ATP content ±3-BrPA. A highly glycolytic hepatocellular carcinoma (HCC) line "AS-30D" [7,8] was used and maintained (Fig. 1A) in female Sprague–Dawley rats (Charles River). For culture, cells ($\sim 1 \times 10^6$) were seeded on a six-well plate in 2 ml RPMI 1640 medium (Invitrogen) containing 10% fetal bovine serum plus 1× antibiotic–antimycotic mixture (Invitrogen) at 37 °C for 3 h in a CO_2 incubator. Hepatocytes ($\sim 1.5 \times 10^6$) were fresh from Cambrex. Cell viability ± 3-BrPA (Sigma) was monitored using the MTT assay (Sigma). For monitoring cell ATP levels, methods of culture using six-well plates and 3-BrPA treatment were as above. Then,

☆ This work was supported by start-up funds to Y.H.K. from the Department of Radiology, by NIH Grants CA 10951 and CA 80118 to P.L.P. and Grant CA92871 to M.G.P.
☆☆ *Abbreviations:* 3-BrPA, 3-bromopyruvic acid; HCC, hepatocellular carcinoma; PET, positron emission tomography; FDG, ^{18}F-2-deoxyglucose.
* Corresponding authors. Fax: +1 410 614 1944.
E-mail addresses: yko@jhmi.edu (Y.H. Ko), ppederse@jhmi.edu (P.L. Pedersen).

0006-291X/$ - see front matter © 2004 Elsevier Inc. All rights reserved.
doi:10.1016/j.bbrc.2004.09.047

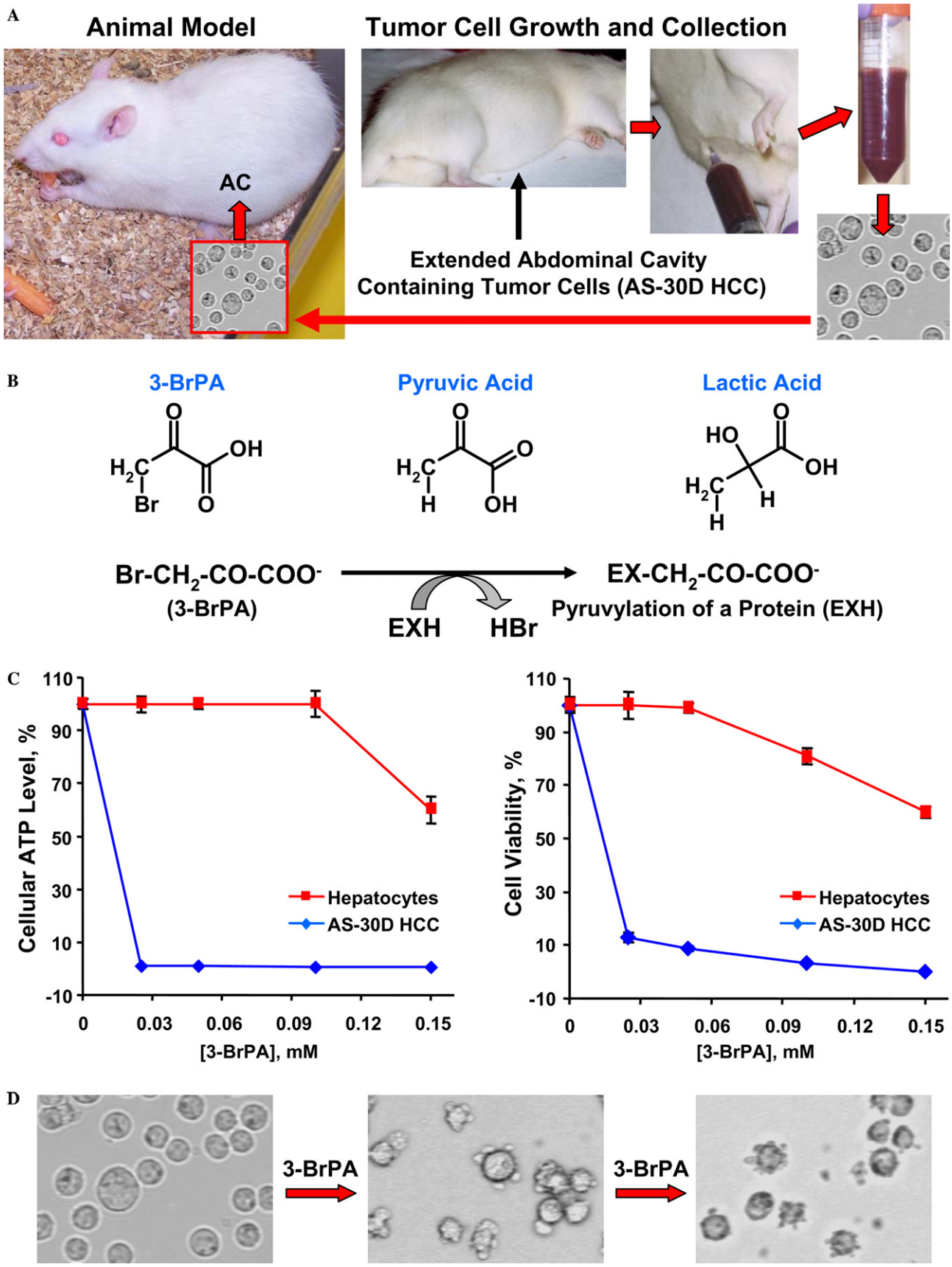

Fig. 1. HCC cells and 3-BrPA. (A) Growth and isolation of HCC cells (AS-30D). (B) Structure and chemical reactivity of 3-BrPA. (C) 3-BrPA-induced depletion of ATP in HCC cells (Left) and loss of viability (Right). (D) Intermediates (Center and Right) in the HCC death pathway.

100 μl aliquots of cells, three for each of the six wells, were removed and transferred into wells of the white culturPlate-96 (Perkin–Elmer). ATP was measured according to Perkin–Elmer using their cell lysate and ATPLite solutions, and Victor 1420 Multilabel Counter.

Induction of advanced cancers and therapy with 3-BrPA. Procedures adhered to Johns Hopkins University Animal Care and Use Committee guidelines. "Advanced cancer" is defined here in the rat as either a collection of HCC cells in the abdominal cavity that cause it to become extended (Fig. 1A) or a solid HCC of 2–3 cm (maximal dimension). To induce ascites tumor cell masses and abdominal tumors, 1 ml, $2–4 \times 10^7$ HCC cells was injected i.p. (Fig. 1A). This resulted in 5–6 days in ~ 40 ml ascites fluid filled with tumor cells (Fig. 1A), and where indicated, also in advanced spherical tumors 2–3 cm in diameter. To induce tumors in the upper back, 1 ml, $2–4 \times 10^7$ HCC cells was injected s.c. Non-spherical tumors of ~ 3 cm (maximal dimension) developed in about 7–10 days. Without treatment, rats hosting HCC cells in ascites form must be euthanized within 7–8 days and in solid form in about 14–21 days. For therapy, animals bearing tumor cells in the abdominal cavity, or together with a spherical tumor (2–3 cm diameter), were treated after 5–6 days with an i.p. injection of 1 ml freshly prepared 2.0 mM 3-BrPA in 1× PBS, pH 7.5, and then for 4 days with the same dosage. The animal named "Two Dottie" also received seven injections of 1 ml of 2.0 mM 3-BrPA on separate days at the tumor site. Those animals bearing tumors 1–2 cm (maximal dimension) in the upper back that were subjected to FDG PET prior to and following therapy were administered eight treatments on successive days with 1 ml of 2 mM 3-BrPA, also in 1× PBS, pH 7.5. Injection of 3-BrPA was into the tumor. The remaining animals containing large tumors (~3 cm maximal dimension) were treated on an individual basis depending on each tumor's responsiveness to 3-BrPA (Table 1).

PET imaging. Rats fasted 12 h with water ad libitum were anesthetized i.p. with 75 mg/kg ketamine and 10 mg/kg xylazine (Abbott Park) in 100–200 μl for induction and subjected to halothane (1% at 1 L/min). FDG (35.0 ± 12.7 MBq, 0.945 ± 0.342 mCi; range 32.7–57.7 MBq, 0.884–1.56 mCi) was injected in the tail vein (10–15 s bolus) in 150 μl. After 45 min, rats were placed in the prone position on the platform of the scanner with the tumor placed within the field-of-view with the aid of laser guidance. An ATLAS small animal PET scanner was used that has an 11.8 cm ring diameter scanner, an 8 cm aperture, a 6 cm effective transverse field-of-view, and a 2 cm axial field of view [9,10]. The imaging system comprised of 18 depth-of-interaction detector modules surrounds the rat. Radial and tangential resolutions of the reconstructed image (pixel size = 0.56 mm) were 1.36 mm at the center, 1.98 (radial), and 2.13 (tangential) at 2 cm radial offset. Sensitivity was >2.0% after correcting for positron escape. Maximal noise equivalent count rate was 10.3 kcps at 52.2 MBq (1.41 mCi) total activity for the rat phantom. These are comparable to those of the prototype scanner used in this study. Images were reconstructed by 3D OSEM [11]. No correction was made for attenuation or scatter. Regions of interest were drawn manually using ATLAS software to encompass the tumor and a region of equal size in the contralateral subcutaneous soft tissues (background). Tumor and background radioactivity were corrected for decay, injected dose, and animal weight, and were expressed in arbitrary units. A paired t test was performed using Microsoft Excel with Analyse-it. P values <0.05 were considered significant.

Histopathology. Tissues were fixed in 10% formalin, sliced at 5 mm intervals, and embedded in paraffin. Sections (4 μm) were stained with hematoxylin and eosin.

Human equivalent of a rat tumor. Tumor location was determined by its position relative to the rat's skeletal anatomy [12] and placed on the human figure using the corresponding skeletal landmarks. Its mass was evaluated by assessing the tumor to body size ratio in the rat and translating this to the human.

Results and discussion

The chemical agent 3-BrPA depletes ATP stores and inhibits HCC cell viability

For therapy, we selected the alkylating agent 3-BrPA [13]. This was based on the hypothesis that because of its

Table 1
History of animals in the advanced cancer treatment/survival study

Animal No.	Animal ID	Group ID	Tumor implantation site	Tumor development area	Method of treatment	Survival time (to date)
1	Star	1	AC	AC	IP	Alive (>1.3 year)
2	Tiny 9	1	AC	AC, LA	IP	(1.3 year)
3	Tip	1	AC	AC	IP	Alive (>1.3 year)
4	One Dottie	1	AC	AC, LA	IP	Alive (>7 months)
5	Two Dottie	1	AC	AC, LA	IP, D	Alive (>7 months)
6	Three Dottie	1	AC	AC, LA	IP	Alive (>7 months)
7 → 12	C1 → C6	1	AC	AC, LA	IP, saline (control)	6–7 days (euthanized)
13 → 20	C7 → C14	1	AC	AC	IP, saline (control)	6–7 days (euthanized)
21	B1	2	UB	UB, S	D, SC, IP	Alive (>7 months)
22	B2	2	UB	UB	D	Alive (>7 months)
23	B6	2	UB	UB, S	D, SC, IP	Alive (>7 months)
24	R1	2	UB	UB	D	Alive (>7 months)
25	R2	2	UB	UB, S	D	Alive (>7 months)
26	R3	2	UB	UB	D	Alive (>7 months)
27	R4	2	UB	UB, S	D, SC, IP	Alive (>7 month)
28	R6	2	UB	UB, S	D, SC	Alive (>7 months)
29[a]	B3[a]	2	UB	UB	D	Alive (>7 months)
30[a]	B4[a]	2	UB	UB	D	Alive (>7 months)
31[a]	B5[a]	2	UB	UB	D	Alive (>7 months)
32[a]	R5[a]	2	UB	UB	D	Alive (>7 months)
33	Sweetie	2	UB	UB	IP	Alive (>7 months)
34	Chubbet	2	None	None	None	Alive (>7 months)

Abbreviations used are: AC, abdominal cavity; LA, lower abdomen; UB, upper back; S, side; IP, intra-peritoneal; SC, subcutaneous; D, direct (locally); and [a]Employed in PET imaging.

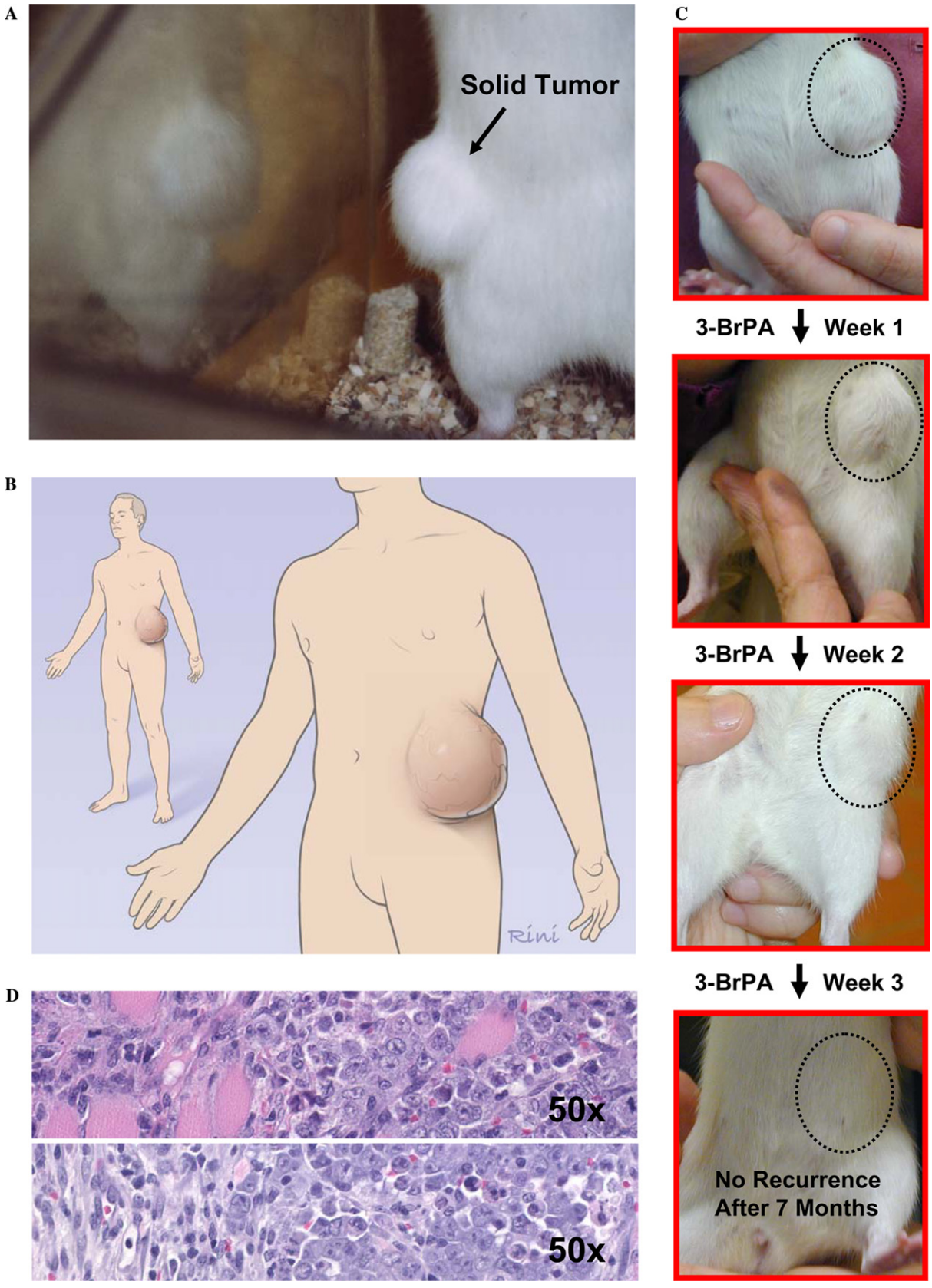

Fig. 2. Complete regression of an advanced abdominal tumor (HCC) after 3-BrPA Therapy. (A) Advanced HCC in "Two Dottie." (B) Human equivalent. (C) Different treatment stages. (D) Tumor histopathology.

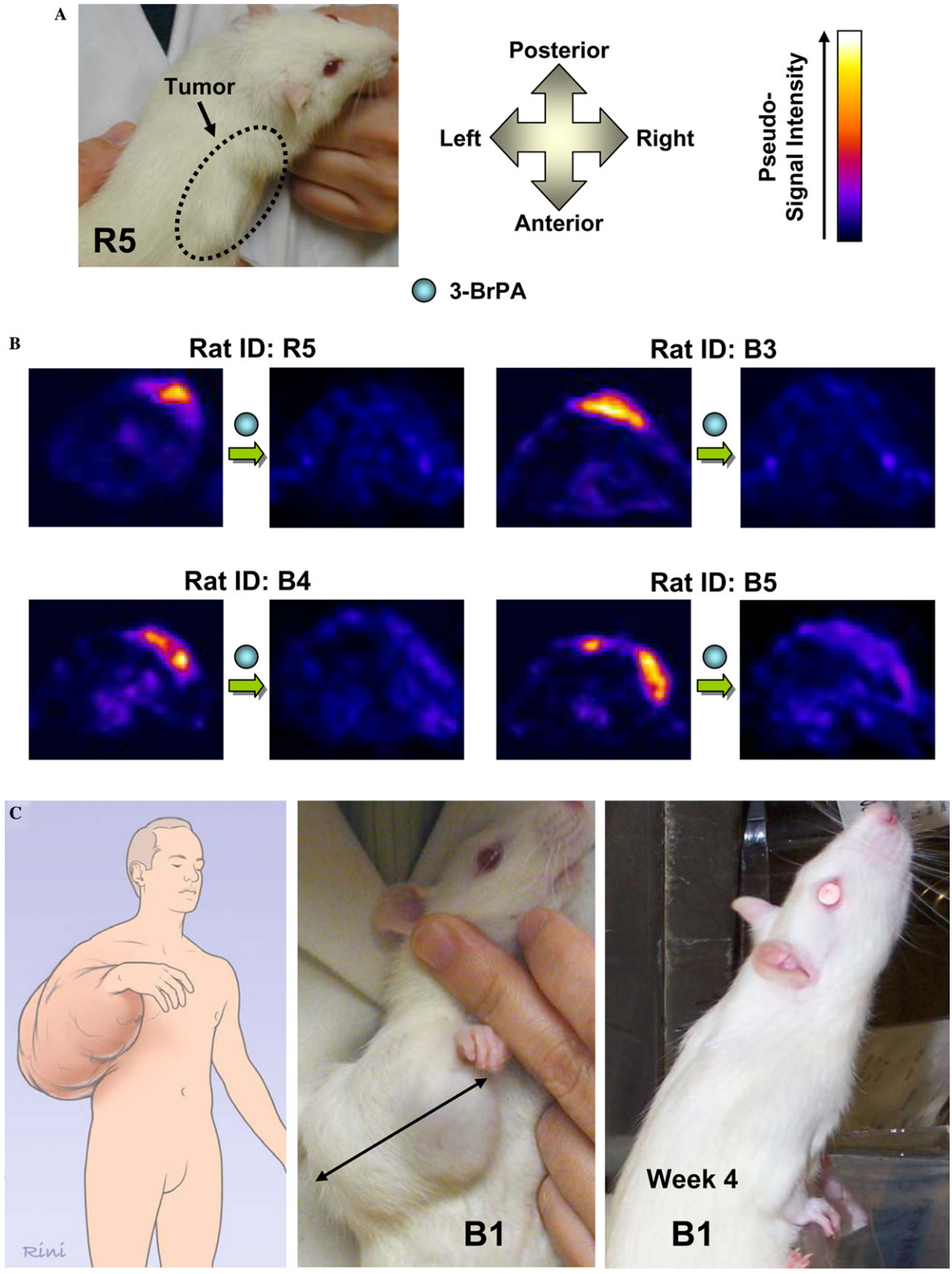

Fig. 3. (A) Preparation for FDG-PET. (Upper left) Rats R5, B3, B4, and B5 were allowed to develop tumors (HCCs). (Upper center) Positional designations for tumors. (Upper right) Pseudo-signal intensity bar. "yellow," increased glucose consumption. (B) FDG-PET images of tumors on R5, B3, B4, and B5 Before and 12 days after 3-BrPA therapy. Therapy involved eight treatments. (C) Rat B1 as one example of nine rats each bearing an advanced tumor (~3 cm) eradicated by 3-BrPA therapy. (Center) Rat B1 bearing a large advanced tumor. (Left) Human equivalent. (Right) Rat B1 one week after 3 weeks of 3-BrPA therapy.

structural similarity to lactate (Fig. 1B), the reactive 3-BrPA may enter cancer cells on the same transporter that exports lactate and then induce ATP depletion. Although earlier work [14,15] showed that 3-BrPA inhibits in vitro the cell's two ATP producing systems, glycolysis and mitochondria, and has antitumor activity, the most critical support for the above hypothesis is presented in Figs. 1C and D. These data show directly that 3-BrPA induces ATP depletion and loss of HCC cell viability. In contrast, hepatocytes show resistance to 3-BrPA. These findings provided support for an ATP depletion-anticancer strategy (see also Supplementary material).

HCC cells growing internally in the abdominal cavity of test animals, and all advanced tumors (HCCs) projecting externally, regressed, and disappeared after 3-BrPA therapy

Table 1 provides information about the 34 female rats in this study divided into Groups 1 and 2. Group 1 animals, named "One Dottie," "Two Dottie," "Three Dottie" "Tiny 9" "Star," and "Tip," had their abdominal cavities filled with rapidly proliferating HCC cells, and the first four also had a spherical tumor (2–3 cm diameter) projecting from their lower abdomen. Fig. 2A shows "Two Dottie" facing her cage revealing the large tumor and its reflection while Fig. 2B presents the predicted human equivalent. "Two Dottie" and the other five animals were treated for five successive days with a single 3-BrPA injection/day into the abdominal cavity. Subsequently, "Two Dottie" also received seven injections on separate days at the tumor site. In 1 week, the extended abdomens regressed in all six animals and in 1 month the tumors completely disappeared. Fig. 2C summarizes the disappearance of the tumor in the abdomen of "Two Dottie." These animals received no additional therapy and showed no tumor recurrence. With the exception of "Tiny Nine" who died tumor free 1.3 years after treatment, the remaining five animals are alive (Table 1). In contrast, all control animals (14 total), treated with saline rather than 3-BrPA, had to be euthanized after only 7–8 days. Histopathology of tumors derived there from showed tumor cell invasion into the abdominal wall (Fig. 2D) with two different cell morphologies, i.e., round and spindled (Fig. 2D).

Moderately advanced tumors (HCCs) growing in the upper backs of test animals also regressed and disappeared following therapy with 3-BrPA, a finding that correlated well with FDG-PET imaging

Results with Group 1 animals gave encouragement to apply 3-BrPA therapy to Group 2 animals bearing tumors in the upper back (Table 1). Of the 13 animals, R5, B3, B4, and B5, the first to develop moderately advanced tumors (Fig. 3A, left), were subjected to FDG-PET. This method allows detection of areas of high glucose consumption [6], and when carried out before and after treatment with 3-BrPA can help assess the extent of metabolic impairment. Trans-axial FDG-PET images (Fig. 3B) of tumors in the upper backs of R5, B3, B4, and B5 prior to treatment with 3-BrPA showed a localized region ("yellow" on the pseudo signal intensity bar in Fig. 1A, right) indicative of increased glucose consumption. In sharp contrast, after a 12 day period in which 3-BrPA was injected directly into the tumor site of each animal on eight different days causing tumor regression and disappearance, the resultant FDG-PET analyses showed no abnormal glucose consumption. Region of interest analysis of those images showed a measurable decrease in glucose consumption by the tumor. Taking all four animals, the decrease in tumor/background radioactivity was significant between the pre- and post-treatment scans ($P = 0.012$). Moreover, there has been no tumor recurrence for >7 months (see also Supplementary material).

All advanced solid tumors (HCCs) growing in the upper backs of test animals also regressed and disappeared following treatment with 3-BrPA

The remaining nine animals in Group 2 (B1, B2, B6, R1, R2, R3, R4, R6, and Sweetie) provided the greatest therapeutic challenge as tumors in each became advanced, i.e., ~3 cm (maximal dimension) and tended to spread to one of the front limbs (Fig. 3C, center, and human equivalent, left). Because of the aggressiveness of these tumors, several treatment approaches with 3-BrPA were investigated (Table 1). Regardless of the approach, further growth of each tumor in the nine animals was arrested, and over a 2–4 week period tumors in all animals regressed and disappeared (Fig. 3C, right, as one example). For >7 months there has been no recurrence (see also Supplementary material for additional examples).

In summary, advanced cancers growing either internally or externally were eradicated in all 19 treated animals using a simple unique ATP depletion strategy, thus providing "proof of principle" that it is possible to defeat quite vicious cancers and spare life at the edge.

Acknowledgments

Drs. Paul Talalay and Donald Coffey are acknowledged for valuable discussions and James Fox and David Blum for technical assistance. Y.H.K. is grateful also to Ilona McClintick and Dr. Ann Morrill for encouragement.

Appendix. Supplementary material

Supplementary data associated with this article can be found, in the online version, at doi:10.1016/j.bbrc.2004.09.047.

References

[1] J. Bruix, L. Boix, M. Sala, J.M. Llovet, Focus on hepatocellular carcinoma, Cancer Cell 5 (2004) 215–219.
[2] O. Warburg, The Metabolism of Tumors, Arnold Constable, London, 1930.
[3] P.L. Pedersen, Tumor mitochondria and the bioenergetics of cancer cells, Prog. Exp. Tumor Res. 22 (1978) 190–274.
[4] P.L. Pedersen, S. Mathupala, A. Rempel, J.F. Geschwind, Y.H. Ko, Mitochondrial bound type II hexokinase: a key player in the growth and survival of many cancers and an ideal prospect for therapeutic intervention, Biochim. Biophys. Acta 1555 (2002) 14–20.
[5] S. Yasuda, S. Arii, A. Mori, N. Isobe, W. Yang, H. Oe, A. Fujimoto, Y. Yonenaga, H. Sakashita, M. Imamura, Hexokinase II and VEGF expression in liver tumors: correlation with hypoxia-inducible factor 1 alpha and its significance, J. Hepatol. 40 (2004) 117–123.
[6] E.M. Rohren, T.G. Turkington, R.E. Coleman, Clinical applications of PET in oncology, Radiology 231 (2004) 305–332.
[7] E. Bustamante, P.L. Pedersen, High aerobic glycolysis of rat hepatoma cells in culture: role of mitochondrial hexokinase, Proc. Natl. Acad. Sci. USA 74 (1977) 3735–3739.
[8] D.F. Smith, E.F. Walborg Jr., J.P. Chang, Establishment of a transplantable ascites variant of a rat hepatoma induced by 3′-methyl-4-dimethylaminoazobenzene, Cancer Res. 30 (1970) 2306–2309.
[9] K. Shimoji, L. Ravasi, K. Schmidt, M.L. Soto-Montenegro, T. Esaki, J. Seidel, E. Jagoda, L. Sokoloff, M.V. Green, W.C. Eckelman, Measurement of cerebral glucose metabolic rates in the anesthetized rat by dynamic scanning with 18F-FDG, the ATLAS small animal PET scanner, and arterial blood sampling, J. Nucl. Med. 45 (2004) 665–672.
[10] S. Siegel, J.J. Vaquero, L. Aloj, J. Seidel, W.R. Gandler, M.V. Green, Initial results from a PET/planar small imaging system, IEEE Trans. Nucl. Sci. 46 (1999) 571–575.
[11] R. Yao, J. Seidel, C.A. Johnson, M.E. Daube-Witherspoon, M.V. Green, R.E. Carson, Performance characteristics of the 3-D OSEM algorithm in the reconstruction of small animal PET images. Ordered-subsets expectation-maximization, IEEE Trans. Med. Imaging 19 (2000) 798–804.
[12] R. Hebel, M.W. Stromberg, Anatomy of the Laboratory Rat, Williams and Wilkins, Baltimore, 1976.
[13] Y.H. Ko, B.A. McFadden, Alkylation of isocitrate lyase from *Escherichia coli* by 3-bromopyruvate, Arch. Biochem. Biophys. 278 (1990) 373–380.
[14] Y.H. Ko, P.L. Pedersen, J.F. Geschwind, Glucose catabolism in the rabbit VX2 tumor model for liver cancer: characterization and targeting hexokinase, Cancer Lett. 173 (2001) 83–91.
[15] J.F. Geschwind, Y.H. Ko, M.S. Torbenson, C. Magee, P.L. Pedersen, Novel therapy for liver cancer: direct intraarterial injection of a potent inhibitor of ATP production, Cancer Res. 62 (2002) 3909–3913.

BBRC Supporting Online Material

ADVANCED CANCERS: ERADICATION IN ALL CASES USING 3-BROMOPYRUVATE THERAPY TO DEPLETE ATP

Young H. Ko, Barbara L. Smith, Yuchuan Wang, Martin G. Pomper, David A. Rini, Michael S. Torbenson, Joanne Hullihen, and Peter L. Pedersen

Supporting Text, Table, and Figures

(See parent manuscript for Table 1 and Figures 1-3.)

ATP Depletion Induced by 3-BrPA in Tumor Cells vs Normal Cells. Data in Fig. 4 further substantiate the selective ATP depletion strategy used in this study to eradicate cancers in all 19 animals studied. (See parent manuscript.) Here, it is shown that when 50 μM 3-BrPA is added to AS-30D HCC cells, known to be highly malignant [1, 2], it completely dissipates cellular ATP levels within 30 min while the same addition to freshly isolated hepatocytes (normal cells) is without effect even after 1.5 h. As indicated in the parent article and supported by an earlier study [3], our hypothesis for the selectivity of 3-BrPA in killing HCC cells is based on the fact that, in contrast to hepatocytes, these cells exhibit the highly glycolytic phenotype [2] common to many cancers [4, 5]. Therefore, the lactate (or similar transporter) is likely to be elevated and unable to distinguish lactate from its reactive structural analog 3-BrPA, thus allowing its entry into the HCC cells and subsequent inhibitory interactions with the ATP producing machinery (glycolysis and mitochondrial oxidative phosphorylation). Considering that the highly glycolytic phenotype is one of the most common to cancers [4], and the basis of one of the most common

techniques to detect them, i.e., FDG-PET [6], then numerous animal and human tumors exhibiting this phenotype are likely candidates in the future for 3-BrPA therapy.

Summary of Data Collected in FDG-PET Analysis of Tumor Regions on the Upper Backs of Animals R5, B3, B4, and B5 Prior to and after Therapy with 3-BrPA. The actual images of the FDG-PET analysis are presented in Fig. 3 of the parent manuscript while Table 2 presented here summarizes the actual data obtained. Here, it can be seen that the subgroup consisting of animals R5, B3, B4, and B5 were subjected to FDG-PET on two separate occasions 12 days apart, i.e., before and after treatment with 3-BrPA. Notably, the SUVs which are indicators of FDG uptake dropped significantly between these two imaging sessions ($p = 0.012$) indicating a substantial treatment effect. Subsequently, this subgroup has survived for more than 7 months and gained weight, further supporting the beneficial effects of therapy with 3-BrPA.

Additional Visual Examples of the Eradication of Advanced Cancers in Animals Studied Here. The tumor (AS-30D HCC) shown in Fig. 5 in the upper back of the animal R4 is clearly advanced occupying not only part of the upper back (upper left panel) but progressing down the right side (upper right panel). Following initial therapy with 3-BrPA, much of the tumor on the upper back is eliminated, and additional therapy eliminates all but a small part of the side tumor (shown in pink/yellow in the middle panels). Hair growing in this area is lost also. Without further therapy, the remaining tumor darkens as it dies completely. Subsequently, the hair lost by R4 returns (bottom panel). The tumor shown in Fig. 6 (upper panel) located partially in the upper back of R6 has extended down the side into a front leg slowing the animal's mobility. Initial therapy with 3-BrPA causes the tumor mass occupying the leg to recede (center left panel) and additional therapy causes the tumor in the upper back to harden (center middle panel) and fall off (right middle panel). Hair then returns (bottom panels). [Photographs by Y.H.K and D.B.]

Photographic Gallery of All 19 Animals that Acquired Advanced Cancers and Were Freed of These Cancers by Treatment with 3-BrPA. The photographs shown in Fig. 7 (A-D) were taken on June 24, 2004 over one year after cancers growing in/on "Star", "Tiny 9", and "Tip" had been eradicated, and 6-7 months after cancers growing on the remaining 16 animals had been eradicated. Chubbet, the 20th animal, served as one of the controls in which cancer was not induced. A group photograph of the same 19 cancer survivors is shown at the bottom of Figure 7D. The individual and group photographs attest to fact that as of June 24, 2004 all 19 animals were alive and active. [Photographs by Norman Barker, Department of Pathology, JHUSOM]

Original and More Recent Weights of All 19 Animals that Acquired Advanced Cancers and Were Freed of These Cancers by Treatment with 3-BrPA. Fig. 8A summarizes both the initial weights of all 19 animals and their weights as of June 24, 2004, while Fig. 8B summarizes the difference. The initial and June 24th weight of Chubbet, a non-cancer control, is shown also. On average the initial weight of all animals was near 180 g, and the average weight gained was 267 g. Therefore, all 19 cancer survivors ate well and grew from early to later adulthood in a normal manner. Today all animals remain healthy and active except "Tiny Nine" who due to complications from ageing was euthanized on July, 26, 2004. She remained tumor free.

Supporting References

1. D. F. Smith, E. F. Walborg, Jr., and J. P. Chang, Establishment of a transplantable ascites variant of a rat hepatoma induced by 3'-methyl-4-dimethylaminoazobenzene, *Cancer Res* 30 (1970) 2306-2309.
2. E. Bustamante, and P. L. Pedersen, High aerobic glycolysis of rat hepatoma cells in culture: role of mitochondrial hexokinase, *Proc Natl Acad Sci U S A* 74 (1977) 3735-3739.

3. Y. H. Ko, P. L. Pedersen, and J. F. Geschwind, Glucose catabolism in the rabbit VX2 tumor model for liver cancer: characterization and targeting hexokinase, *Cancer Lett* 173 (2001) 83-91.

4. O. Warburg, The Metabolism of Tumors, Arnold Constable, London (1930).

5. P. L. Pedersen, S. Mathupala, A. Rempel, J. F. Geschwind, and Y. H. Ko, Mitochondrial bound type II hexokinase: a key player in the growth and survival of many cancers and an ideal prospect for therapeutic intervention, *Biochim Biophys Acta* 1555 (2002) 14-20.

6. G. Jerusalem, R. Hustinx, Y. Beguin, and G. Fillet, PET scan imaging in oncology, *Eur J Cancer* 39 (2003) 1525-1534.

Figure Legends And Table 2

(See parent manuscript for Figures 1-3.)

Figure 4. Comparison of the Effect of 3-BrPA on the ATP Content of Hepatocytes (Normal Cells) and AS-30D HCC cells as a function of time. Experiments were carried out exactly as described under ***Materials and Methods*** in the parent manuscript. Both fresh intact hepatocytes and AS-30D HCC cells were exposed to 50 μM 3-BrPA for the times indicated, after which they were subjected to ATP content analysis also as described under ***Materials and Methods*** in the parent manuscript.

Figure 5. Response of an Advanced Tumor (AS-30D HCC) in the Upper Back and Right Side of the Animal R4 to Treatment with 3-BrPA. As indicated in Table 1 of the parent manuscript, the animal R4 received at different times direct, subcutaneous, and intraperitoneal injections of 3-BrPA causing the large tumor (upper photographs) to first recede and form an open wound-like area (center photographs), and finally to heal with replacement of lost hair.

Once healed (in about one month), no further therapy was applied and there has been no recurrence of the tumor for over 7 months (bottom photograph).

Figure 6. Response of an Advanced Tumor (AS-30D HCC) in the Upper Back and Left Front Limb of the Animal R6 to Treatment with 3-BrPA. Here the mobility of R6 has become partially impaired. As indicated in Table 1 of the parent manuscript, R6 received at different times direct, and subcutaneous injections of 3-BrPA but no intraperitoneal injection. Within one month, the large tumor had regressed completely and R6 regained full mobility of her left front limb. As for R4 above, no further therapy was applied and there has been no recurrence of the tumor for over 7 months.

Figure 7. Individual Photographs of Each of the 19 Cancer Survivors and of One of the Non-Cancer Controls (Chubbet). Photographs were taken on June 24, 2004 over one year after advanced cancers growing in/on "Star", "Tiny 9", and "Tip" had regressed and disappeared in response to 3-BrPA therapy, and 6-7 months after advanced cancers on the remaining 16 animals had disappeared. To date, there has been no tumor recurrence in any of the remaining animals. A group photograph of all 19 cancer survivors is shown at the bottom of Fig. 7D.

Figure 8. A. Initial Body Weight (light shading) and Weight on June 24, 2004 (dark shading) of the 19 Cancer Surviving animals, and of the Non-Cancer Control (Chubbet). The initial average weight of all animals upon arrival was 180 g. **B. Summary of Body Weight Gain.** On average the animals gained 267 g since their arrival. There has never been a loss of appetite or weight observed for any of the animals during the course of this study. As indicated above Tiny 9 has since passed away of age-related causes but remained tumor-free.

Table 2
(See parent manuscript for Table 1.)

FDG-PET Analysis

Subject	Study	Weight (g)	SUV_t	SUV_b	$SUV_{t/b}$
R5	1	201	97.4	14.3	6.8
	2	238	13.8	9.7	1.4
B3	1	208	30.6	6.4	4.8
	2	240	10.5	4.5	2.3
B4	1	200	48.3	6.0	8.1
	2	229	11.3	8.3	1.4
B5	1	206	18.2	2.7	6.9
	2	238	10.5	5.9	1.8
Average	1	204 ± 4	--	--	6.6 ± 1.4
	2	236 ± 5	--	--	1.7 ± 0.4

Studies 1 and 2 were performed 12 days apart; SUV_t and SUV_b are standardized uptake values for tumor and background, respectively (arbitrary units).

Figure 4

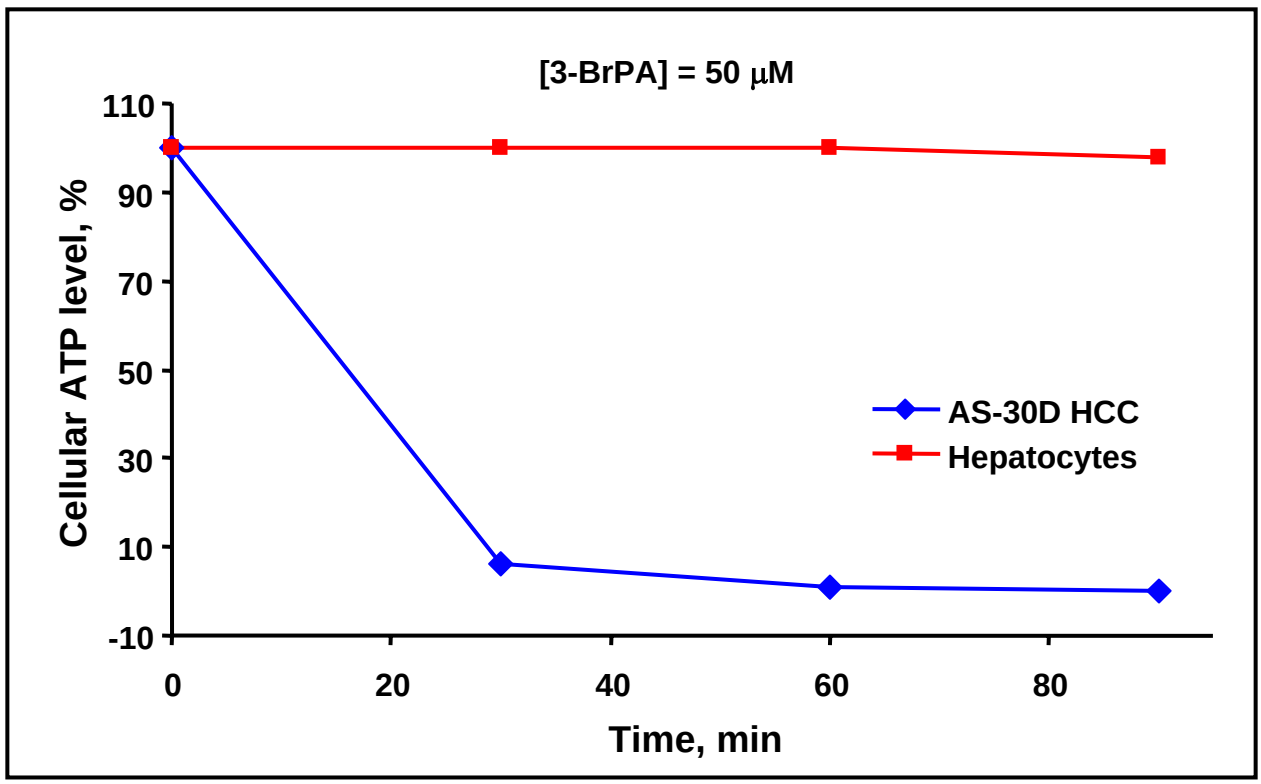
[3-BrPA] = 50 μM
Cellular ATP level, %
110
90
70
50
30
10
-10
0
20
40
60
80
Time, min
AS-30D HCC
Hepatocytes

Figure 5

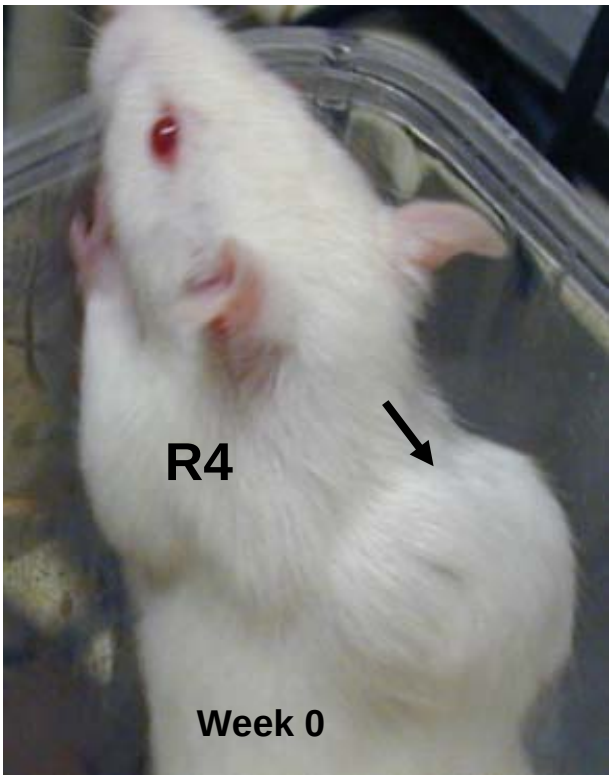

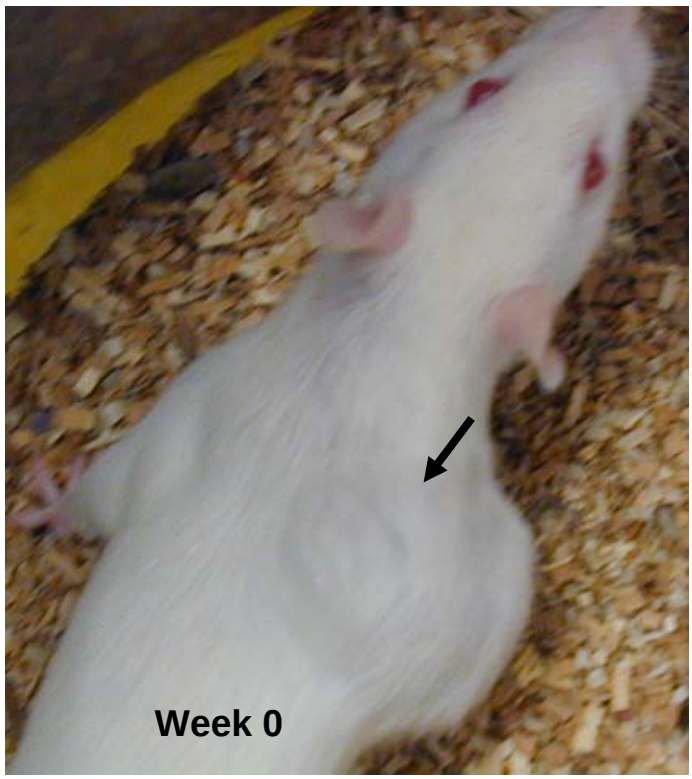

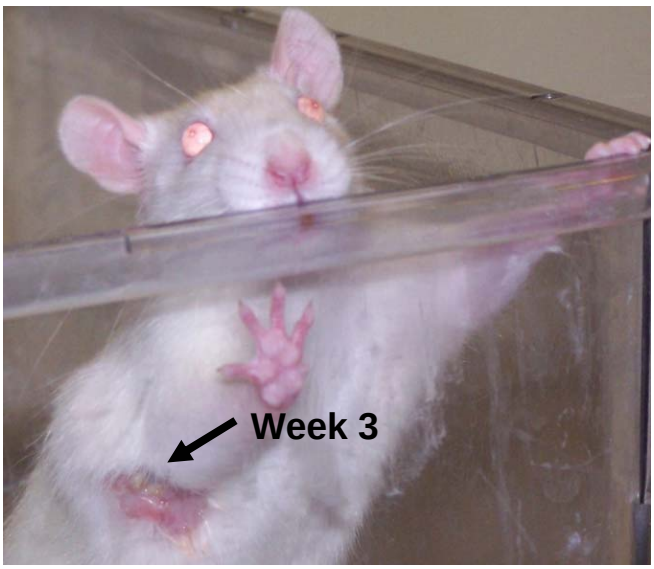

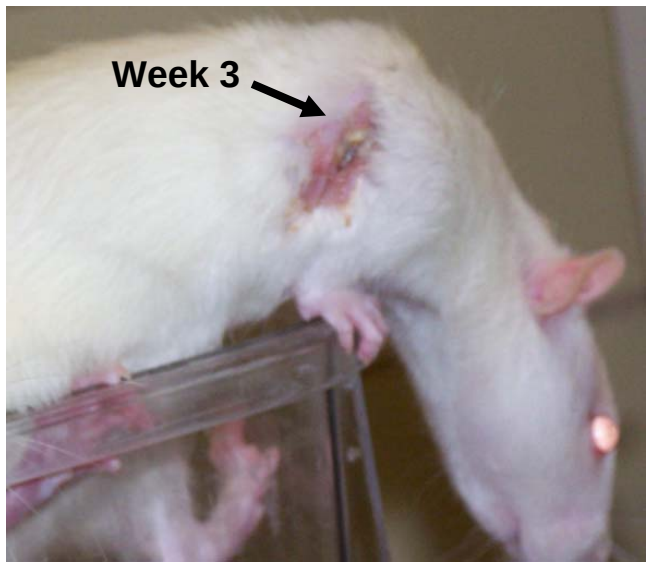

Figure 6

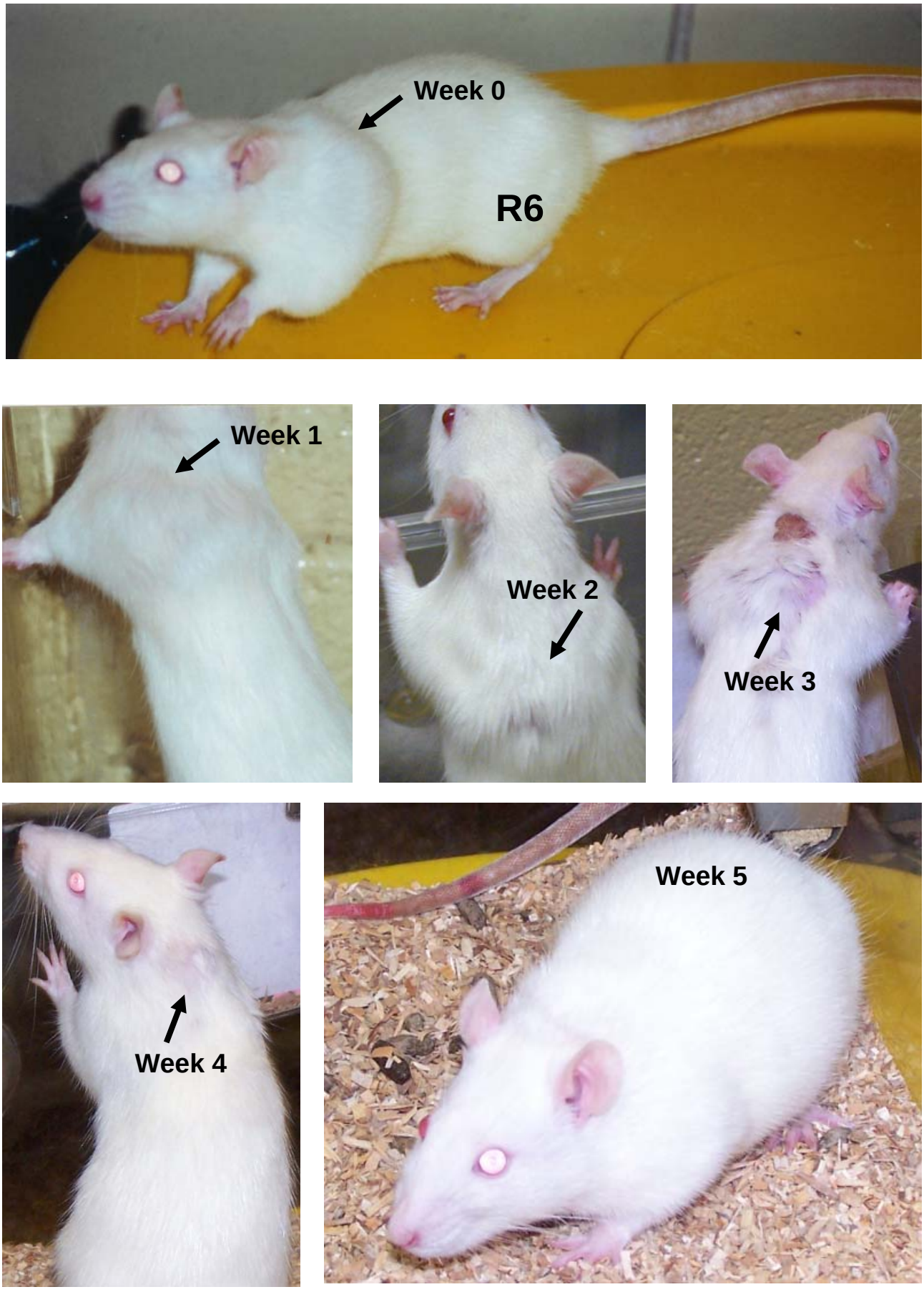

Figure 7A

B1

B2

B3

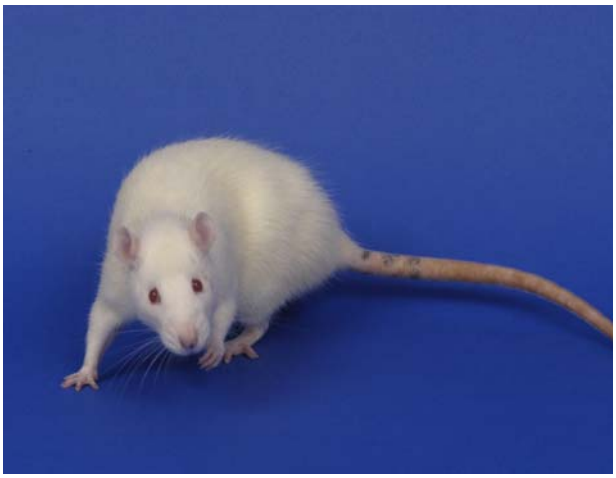

B4

B5

B6

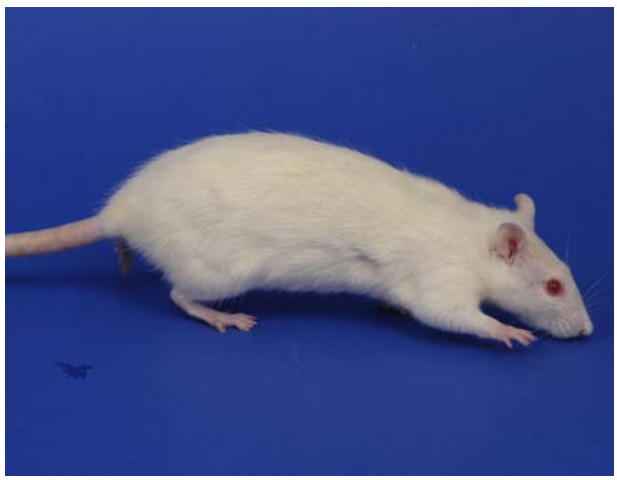

Figure 7B

R1

R2

R3

R4

R5

R6

Figure 7C

One Dottie

Two Dottie

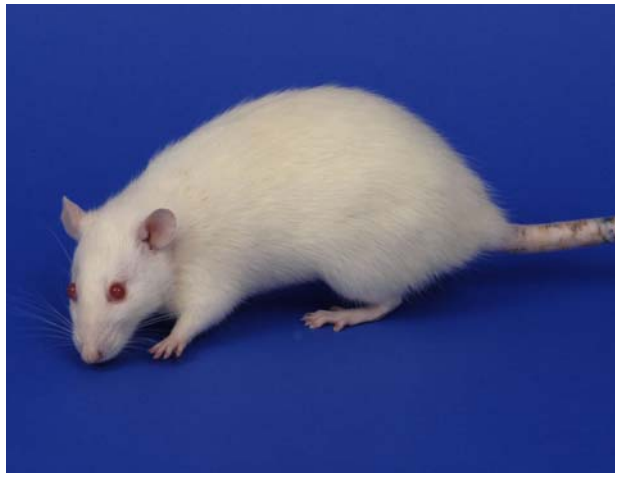

Three Dottie

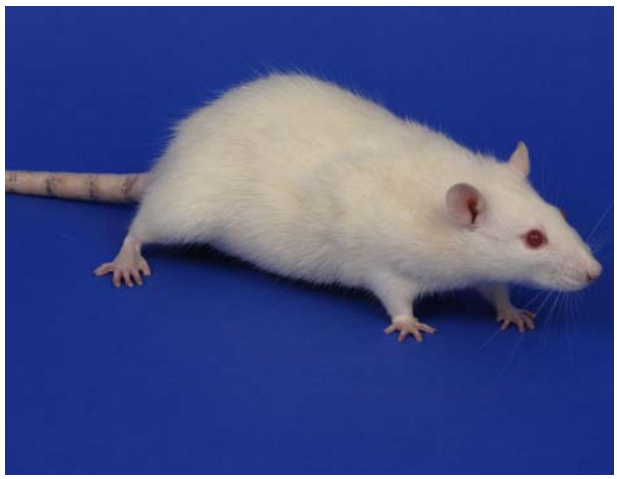

Star

Tip

Tiny 9

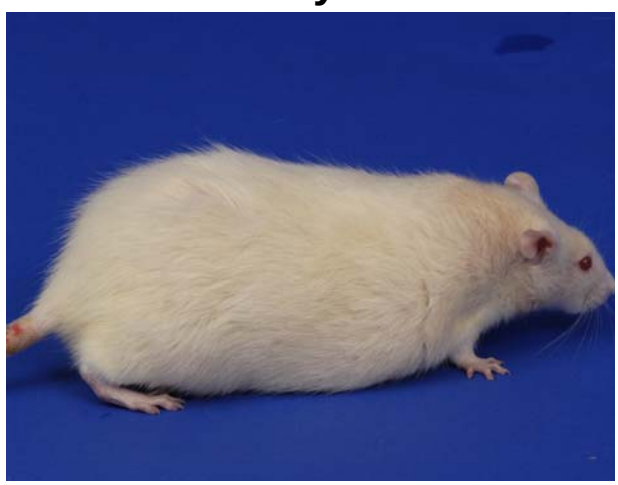

Figure 7D

Sweetie

Chubbet

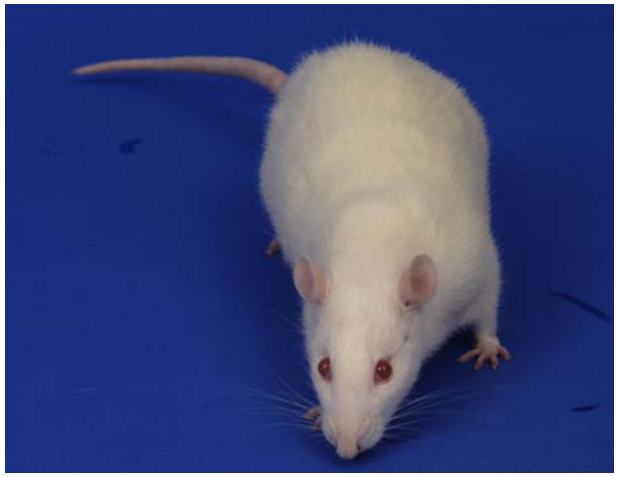

Cancer Survivors (Group Photo)

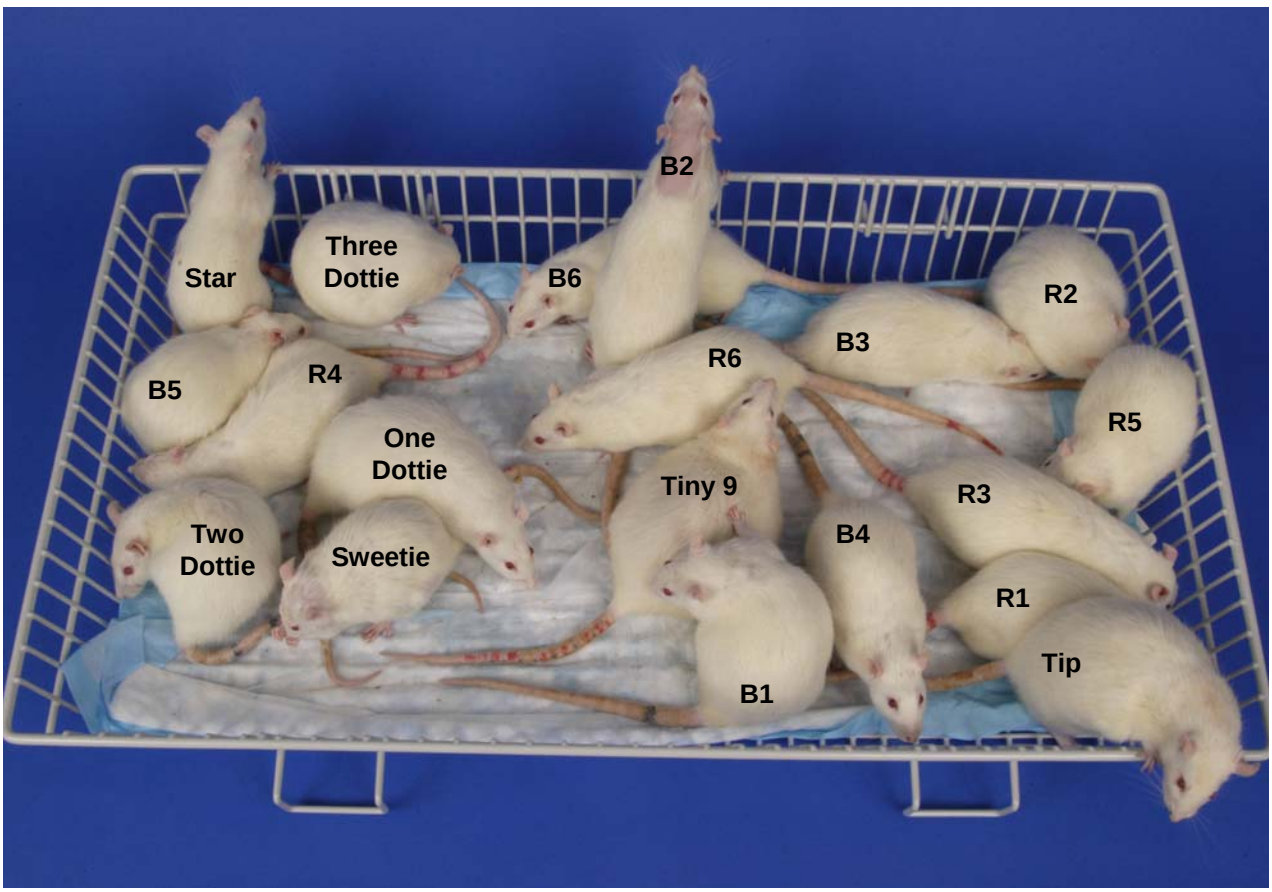

June 24, 2004

Figure 8

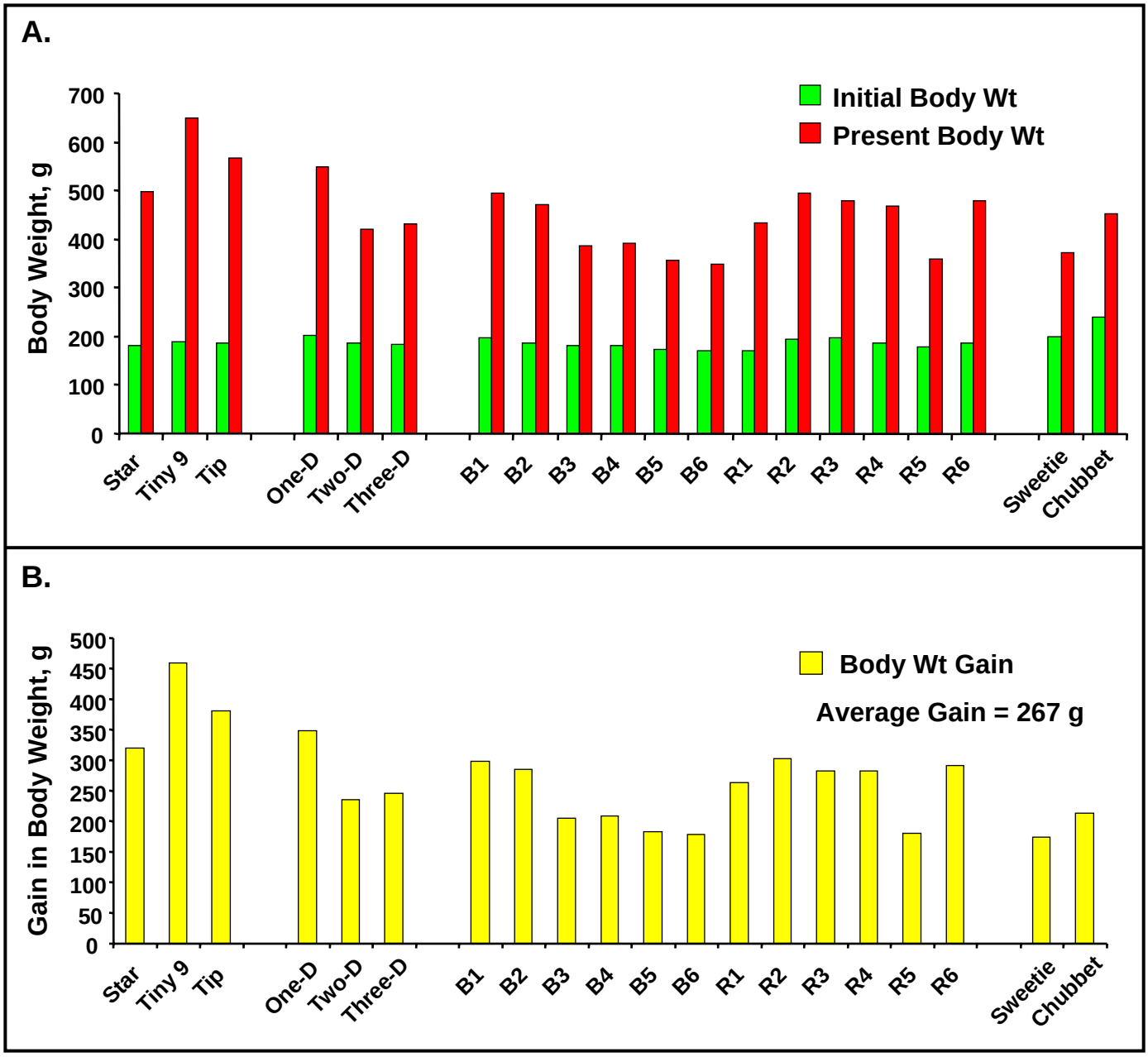
A.
Body Weight, g
700
600
500
400
300
200
100
0
Initial Body Wt
Present Body Wt
Star
Tiny 9
Tip
One-D
Two-D
Three-D
B1
B2
B3
B4
B5
B6
R1
R2
R3
R4
R5
R6
Sweetie
Chubbet
B.
Gain in Body Weight, g
500
450
400
350
300
250
200
150
100
50
0
Body Wt Gain
Average Gain = 267 g
Star
Tiny 9
Tip
One-D
Two-D
Three-D
B1
B2
B3
B4
B5
B6
R1
R2
R3
R4
R5
R6
Sweetie
Chubbet